Construction and Building Materials 351 (2022) 128948

Contents lists available at ScienceDirect

Construction and Building Materials

journal homepage: www.elsevier.com/locate/conbuildmat

Crushing effects on the durability of rocky aggregates used on road surfaces subjected to winter maintenance and extreme climate conditions

A.P. Pérez-Fortes [a,*], M.J. Varas-Muriel [b,c], M. Bermejo [d]

[a] Department of Civil Engineering Construction, E.T.S I. de Caminos, Canales y Puertos, Universidad Politécnica de Madrid, C/Profesor Aranguren, s/n, 28040 Madrid, Spain
[b] Geological Sciences Faculty, Complutense University of Madrid, C/Jose Antonio Novais, 12, 28040 Madrid, Spain
[c] Geosciences Institute (UCM, CSIC), C/Doctor Severo Ochoa 7, 28040 Madrid, Spain
[d] Department of Engineering, Aviation and Technology. Saint Louis University, Avenida del Valle, 34, 28003 Madrid, Spain

ARTICLE INFO

Keywords:
Aggregates
Rocks
Porosity
Durability
Quarry
Road surfaces
Salts
Winter maintenance
Extreme climate

ABSTRACT

The internal structure of a rock is determined by its empty spaces (pores and cracks), which can evolve over time by chemical, physical, or biological processes. In construction, these chemical and physical processes, and their effects in the final products, known as aggregates, are well known, and controlled to estimate their quality and durability. However, the intrinsic properties of the raw material, the rock, and the processes that can affect its quality and durability during the production of the aggregates are poorly studied and considered in construction. For this reason, the evolution of the internal structure of two different types of aggregates used in Spanish roads were analyzed. The aggregates will be also studied in their raw form, rock, by measuring their water absorption coefficient and using mercury porosimetry and fluorescence microscopy. To estimate the influence of the internal structure in the durability of the aggregates, both forms, rocks, and aggregates, will be subjected to the combined effect of temperature variations and the salt used during winter maintenance operations on Spanish roads. The results obtained show that crushing processes in the quarry increase the water absorption coefficient of both materials and generate new micro-porosity caused by the microcracking of weak areas of the rock such as its schistosity or the presence of previous cracks. Thus, this increasing of the porosity produced by crushing processes in the quarry has a negative impact on the durability of the aggregates when they are subjected to winter maintenance operations and extreme climate conditions.

1. Introduction

Rocks are materials traditionally used in construction, either as natural stone in blocks or well crushed as aggregates due to their resistance and durability [1]. This resistance and durability depends on the mineral components of the rock (mineralogy), their spatial distribution and grain or crystal size (texture), and the presence of empty spaces such as pores and fissures (internal structure) [1–5]. In this way, the internal structure is directly responsible for the hydric behavior (permeability, water absorption) as well as the durability of rocks and, ultimately, rocky aggregates [4].

It is well known that the porous media and its saturation state are the main cause of rocks' frost resistance [6–10], salt crystallization damaging [11–14] or, in lower levels, microbial deterioration [15–19] since they contain the fluids and the solid–fluid contact where chemical alteration reactions and microbial populations take place. Therefore, the durability of those aggregates formed by rocks is also dependent of the properties of their porous media (pore size and its distribution, pore shape, and connectivity). Rocks and rocky aggregates with small pore sizes (<5 μm), where water cannot move freely, tend to be rapidly deteriorated by water itself, freeze-thawing processes, or de-icing salts [4,20–22]. The shape of the pores is also an important parameter to control the amount of water that rocks and therefore, rocky aggregates, can absorb or store [23]. Additionally, rocks and aggregates with smaller and more irregular pores result in a larger specific surface area that is exposed to physical, chemical, or biological agents of deterioration. Equally, the connectivity between pores is one of the main factors that control the permeability and water absorption in rocks and

* Corresponding author at: Dept. Civil Engineering: Construction, Campus Ciudad Universitaria, Calle del Prof. Aranguren, 3, Laboratory of Construction Materials (Basement -1). 28040 Madrid, Spain.
E-mail addresses: anapatricia.perez@upm.es (A.P. Pérez-Fortes), mjvaras@ucm.es (M.J. Varas-Muriel), mario.bermejocastro@slu.edu (M. Bermejo).

https://doi.org/10.1016/j.conbuildmat.2022.128948
Received 30 March 2022; Received in revised form 1 August 2022; Accepted 21 August 2022
Available online 2 September 2022

aggregates [4]. In this way, it is considered that rocks having <2 % of water absorption coefficient produce high quality and durable aggregates. By contrast, rocks with >4 % of water absorption coefficient generate poor quality and low durable rocky aggregates [4,24,25].

On the other side, the different deterioration agents of the aggregates used on roads can be organized in three different manufacturing states: aggregate production, road construction, and road commissioning [26,27]. In the production stage, rocks and aggregates can be physically deteriorated by blasting and crushing processes in the quarry [27–30]. During road construction, aggregates are mainly physically deteriorated by the heating processes necessary to produce asphalt mixtures and the compaction of these mixtures to generate the asphalt pavements [27,31]. Finally, it is well known that, during roads' commissioning, asphalt binder is rapidly degraded, exposing the aggregates to physical and chemical deterioration processes [32,33]. These processes can be caused by natural agents, especially related to environmental conditions such as rainfall, ice/snow, or insolation [26,27] and anthropogenic agents, especially related to traffic loads and the presence of pollutants [27].

In this context, the aggregates used on Spanish road surfaces are subjected to several specifications to control their quality and durability [34,35]. These specifications cover the necessary properties of the aggregates to fabricate good quality asphalt pavements during road construction. These properties can be their morphology [36] or their affinity with asphalt binders [37]. Equally, these specifications control the durable behavior of the aggregates, considering environmental agents of deterioration such as freeze-thawing [38] and thermal stress [39] or anthropogenic agents of deterioration like traffic wearing [40]. However, there is still a lack of information about these properties and especially the mechanisms of deterioration of the aggregates during their extraction and production. Although several authors have studied the crushing and crusher effects on the morphology and mechanical resistance of aggregates, e. g. [41–48], not many works have been published considering the impact of these effects on aggregates durability [28,29,49]. In this sense, the link between rock (geology origin) and aggregates' properties, is also still underestimated [33]. For instance, a deep knowledge of the quality and durability of the rocks forming aggregates may help, for instance, to develop future models to predict aggregates quality and durability from quarry faces regarding processing effects such as crushing.

For these reasons, in this paper, the internal structure of two types of rocks used as crushed aggregates on Spanish road surfaces (wearing courses) is studied. Pore size and shape of both samples are obtained with mercury porosimetry, while pore connectivity is determined by the samples' water absorption capacity and fluorescence microscopy. In addition, to estimate the evolution of the internal structure due to crushing effects in the quarry, both types of rocky materials are analyzed, not only in their raw state, rock, but also in their product form, aggregates. The aim to analyze both states, rock, and aggregate, is to determine relationships between rock type (geology), processing method (crushing) and environmental conditions (durability). Regarding the environmental conditions, both materials are used on road surfaces located near Santiago de Compostela, in the NW of the Iberian Peninsula. This area has a humid and mountainous climate [50]. However, cold and heat waves in particular are becoming more frequent in the area in the last decades due to local deforestation and global warming [51–54]. Thus, the effects of crushing processes in the durability of the aggregates are also evaluated, considering the adverse actions of winter (freeze-thawing) and summer (thermal stress).

Finally, it must be highlighted that the roads where these rocky aggregates are provided are commonly subjected to winter maintenance operations. As salt (NaCl) is the substance frequently used in Spanish winter maintenance operations to reduce the freezing point of water, this element has been included in the development of laboratory durability tests. Hence, it is well known that NaCl is directly responsible for the deterioration of road surfaces [50,55–59]. Additionally, it was considered that in summer, the salt spread during winter can remain on the pavement or be dissolved by rain and deposited in adjoining areas [60–63]. Thus, in addition to the effect of high temperatures, NaCl can continue with the degradation of the material in a short period of time. Therefore, the deterioration effects of the most common deicer used in Spain, NaCl has been included in this work.

2. Materials and methods

The materials selected are schist and amphibolite exploited in a quarry from the northwest of Spain, near the city of Santiago de Compostela (Fig. 1). This quarry makes use of the abandoned vertical cuts of an old ore copper sulfide deposit [30,64,65], and it is formed by four open benches, three of them operational during the collection of the samples. The samples of rock were taken in the operational benches after extraction works by blasting (Fig. 1). The aggregates, produced by the primarily rock crushing by a gyratory crusher and the secondly crushing process by impact crushers, were taken from the production stockpiles of the quarry (Fig. 2)Thus, the aggregates collected corresponded to the same crushed stone sampled in the quarry face.

The density measured in the production plant of schist aggregates is 2850 kg/m^3, while the density of amphibolite aggregates is 3080 kg/m^3. In accordance, Los Angeles resistance (LA) measured in the plant for schist aggregates is 18, while the measurement for amphibolite aggregates is 9 [30]. Polished Stone Value (PSV) of amphibolite aggregate is 41 while PSV of schist aggregate is 53 [50]. Although both materials meet Spanish physical and mechanical requirements to be used on wearing courses [35], regarding road classification, both lithologies can be mixed to form aggregates with two parts of amphibolite per each part of schist to improve the polish resistance.

Rock samples collected from the quarry benches were cut in the laboratory to obtain, in total, 20 cubic blocks with dimensions 7 × 7 × 7 cm, 10 cubic blocks per each lithology, schist, and amphibolite (Fig. 2a). Other minor fragments of the rock were used to perform the petrographic analysis of both lithologies. Aggregate samples were obtained from different points of the stockpiles, at an intermediate height and at least 200 mm below its surface [24] to avoid the segregation of sizes that occurs when the aggregate falls from the conveyor belt to the gathering. 120 kg of aggregates with particle size distribution 12/18 (60 kg per each type of rock) and 100 kg of aggregates with particle size distribution 6/12 (50 kg per each lithology) were collected. The aggregates sampled were prepared according to EN 932-1 [66] and EN 1097-2 [67], to obtain, in total, 30 kg of crushed aggregates with particle sizes 10/14 mm [67], 15 kg per each lithology, schist, and amphibolite, and 12 kg of crushed aggregates with particle sizes 6/12 mm were taken, 6 kg per each lithology (Fig. 2b). The nomenclature and subsamples of the rock and aggregate samples are respectively shown in Tables 1 and 2.

The samples shown in Tables 1 and 2, were analyzed with the different techniques and tests described below before and after the durability tests also shown below. Thus, the evolution of the internal structure of the rock and aggregates regarding the environmental conditions of the road is assessed by the comparison between the properties of the material untreated in the laboratory and the material treated with the durability tests in the laboratory. Thereby, the influence of rock crushing and environmental conditions is stablished.

2.1. Water absorption coefficient

The water absorption coefficient of rocky blocks (Table 1) was measured following the EN 13755 procedure [68] and using a balance with ±0.01 g accuracy. The blocks, previously dried up to constant weight (W_d), are placed in a container where distilled water is introduced up to half the height of the specimens (t_0). After 1 h, more distilled water is added until reaching three quarters of the height of the specimens, and after 2 h of testing, more water is added until the specimens are completely submerged. The samples remain submerged for 72 h and,

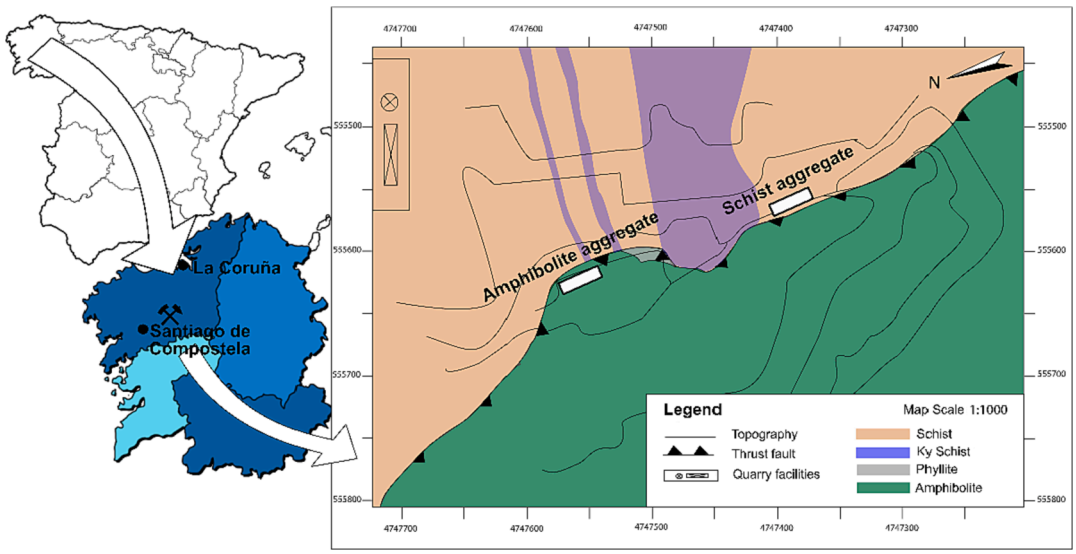

Fig. 1. Location and schematic geology of the studied quarry. Rock samples and aggregates were collected in the areas marked with white rectangles [50].

Fig. 2. Sampling working face on the left and stockpile on the right of the studied quarry.

Table 1
Distribution and nomenclature of the rocks used.

Type	Sample	Lithology	Units	Nomenclature								
Rock	Cubic blocks	Amphibolite	10	A1	A2	AFT1	AFT2	AFT3	AFT4	ATS1	ATS2	ATS3	ATS4
		Schist	10	S1	S2	SFT1	SFT2	SFT3	SFT4	STS1	STS2	STS3	STS4

Table 2
Distribution and nomenclature of the aggregates used.

Type	Particle Size	Lithology	Sample	Subsample	Subsample's Nomenclature		
Aggregate	10/14 mm	Amphibolite	15 kg	5 kg	AALA	AAFTLA	AATSLA
		Schist	15 kg	5 kg	SALA	SAFTLA	SATSLA
	6/12 mm	Amphibolite	6 kg	2 kg	AA	AAFT	AATS
		Schist	6 kg	2 kg	SA	SAFT	SATS

after this time, the saturated weight (W_s) is registered, and the water absorption coefficient (C_{Abs}) calculated following Eq. (1):

$$C_{Abs} = \frac{(W_s - W_d)}{W_d} \times 100 \quad (1)$$

The water absorption coefficient of the aggregates (Table 2) was measured according to EN 1097-6 method [69] with the same balance. Primarily, the aggregate samples are dried up to gain constant weight (W_d) and, subsequently, they are placed in trays where they are submerged in distilled water for 24 h. After this time, the saturated samples are weighed (W_s), obtaining their water absorption coefficient with Eq. (1).

In addition, the rock and aggregate samples were measured while saturated and submerged in distilled water with a hydrostatic balance (W_h) with ± 0.01 g accuracy to estimate their *relative density* (d_r) and *open porosity* (P_w, [70], Eqs. (2) and (3)):

$$d_r = \frac{W_d}{W_d - W_h} \times \rho_w \quad (2)$$

$$P_w = \frac{W_s - W_d}{W_s - W_h} \times 100 \quad (3)$$

where ρ_w is water density at 20 °C.

2.2. Mercury porosimetry

Mercury porosimetry consists of introducing mercury under pressure into the porous system of a material with the aim to determine the volume of mercury that enters the different types of pores at different pressures to represent an intrusion curve from which the pore size distribution of the tested material is obtained, according to Washburn Law (Eq. (4), [71,72]).

$$P = \frac{-2\gamma cos\theta}{r} \quad (4)$$

where P is the intrusion pressure; r is the radius of the cylindrical pore intruded; γ is the surface tension of the mercury; θ is the contact angle between the mercury and the pore wall.

Mercury porosimetry was applied to fragments cut from the rock blocks (Table 1) and some particles of the 6/12 aggregate samples (Table 2), following the ASTM D 4404-18 test procedure [73]. The equipment used was a porosimeter from Micromeritics, model Autopore IV 9500, whose pore size range is 0.001–1000 μm and the mercury pressure exerted for the intrusion reaches 60,000 psi. Finally, the parameters calculated are the apparent and relative density of the rock and aggregate samples, their total percentage of porosity, the shape of the pores, the distribution of the different pore sizes, and the macroporosity/microporosity relationship. The limit between macro and microporosity was established at 5 μm of pore diameter and the shape of the capillary connections were defined using tortuosity parameter [20,74,75].

2.3. Polarized light optical (OM) and fluorescence microscopy (FM)

Polarized Light Optical (OM) and Fluorescence Microscopy (FM) were also measured in fragments cut from the rock blocks and some particles of the aggregate samples. OM is a technique based on the observation and recognition of minerals and their textural relationships in rocks, including their internal structure [76]. By contrast, FM is applied to non-fluorescent substances such as most rock lithologies and facilitates internal structural observations, highlighting important characteristics such as porosity, micro-cracks, and fissures, which sometimes present certain problems to be analyzed with OM [77]. With this purpose, a resin with a fluorescent colorant must be infiltrated in the rock, filling its porosity.

With the aim to perform the OM and FM analyses of the rock and aggregate samples, 12 thin sections, with dimensions of 3 × 2 cm and 30 μm thickness, were prepared in the laboratory. From these 12 thin sections, 6 sections were prepared from rocky blocks (Table 1), 3 sections per each type of lithology; the other 6 sections were prepared from 6/12 aggregate samples (Table 2), 3 sections per each type of lithology.

Finally, the equipment used was an Olympus BX51 model polarized light optical microscope with four magnifications (×4, ×10, ×20 and ×50), camera coupled Olympus DP12 model (6 V/2.5 Å), and Olympus DP-Soft Version 3.2 image download software.

2.4. Durability Tests: Freeze-thawing and thermal stress

Due to the final use of the aggregates studied on road surfaces from mountain areas with contrasting climatology, the chosen test procedures tried to evaluate the behavior of the material exploited in the quarry against the action of water, extreme low temperatures in winter (freeze-thawing), and extreme dryness with high temperatures in summer (thermal stress). As it has been previously introduced, NaCl is the winter substance most frequently used in Spanish winter maintenance operations on roads, and therefore, this element was included in the development of the durability tests in the laboratory.

In total, 8 rock blocks, 4 blocks per each type of lithology (Table 1), and 4 kg of aggregates, 2 kg per each type of lithology (Table 2), were subjected to freeze–thaw tests [38]. Prior to the tests, the mentioned samples were dried to a constant weight. Afterwards, the samples were submerged in a saturated brine of NaCl for 48 h. Once the samples were saturated in NaCl brine, they were frozen for 16 h at −21 °C and thawed submerged in the same NaCl brine at room temperature (20 ± 3 °C) for the remaining 8 h. This process was repeated 70 times.

Similarly, in total, 8 rock blocks, 4 blocks per each type of lithology (Table 1), and 4 kg of aggregates, 2 kg per each type of lithology (Table 2), were subjected to thermal stress tests [39]. The samples were also submerged in a saturated NaCl brine for 48 h to ensure their saturation before beginning the test. Afterwards, the samples were heated to 110 ± 5 °C for 6 h and submerged in the same NaCl brine at room temperature (20 ± 3 °C) for the remaining 18 h. This process was repeated 40 times.

After the durability tests, the samples were weighed to assess their percentage weight loss, comparing their initial (W_0) and final weight (W_f). Afterwards, aged samples were cleaned in distilled water, and the water absorption coefficient test, mercury porosimetry and OM and FM analyses were again performed to estimate the evolution of the internal structure of both lithologies regarding crushing processes and road environmental conditions. With this purpose, the water absorption coefficient was measured directly on the aged samples. By contrast, to measure with mercury porosimeter and prepare the thin sections for the OM and FM analyses, small fragments of rock were cut from 0.5 cm of the rock samples' surface. Equally, some particles from the aged samples of aggregates were used in the mercury porosimetry and OM and FM analyses.

3. Results

Before the tests and analyses were performed, a visual inspection on the rock and aggregate samples before and after the durability tests was done. The schist has a foliated structure with a medium to coarse grain size (Fig. 3a–c). Dark domain of schist is the finest grain size while light domain is the coarsest grain size. Related with these light bands, metallic minerals that could correspond to sulfides are observed. These minerals sometimes appear oxidized, giving rise to reddish or orange colors. Additionally, quartz veins with millimeter thicknesses usually cross this lithology perpendicularly to the main foliation. By contrast, amphibolite has a very fine grain size (Fig. 3d, e). In appearance, it is a massive rock where millimeter-thick bands cross the rock with different orientations and light minerals. Associated with these bands, there are metallic minerals that could correspond to sulfides. Occasionally, minerals with reddish to orange tones are also associated with these bands, indicating that these sulfides have oxidized, giving rise to oxides and hydroxides.

After the freeze-thawing test in the laboratory of rock blocks (Fig. 3b and e), schist samples showed a slight reddish coloration due to the oxidation of sulfides, where possible oxides present in the rocks had a greater reddish intensity in the quartz-feldspar domains. This coloration was also noticed in the opening and enlargement of pre-existing fissures and the formation of new ones in general, parallel to the foliation of the rock and associated with the contact between the micaceous and quartz-feldspathic domains (Fig. 3b). Occasionally, new fissures perpendicular to the main foliation of the rock were also observed, possibly related to quartz veins (Fig. 3b). Equally, in amphibolite rock samples, the opening of pre-existing fissures and the formation of new ones (Fig. 3e) were observed. These fissures were both parallel and perpendicular to the

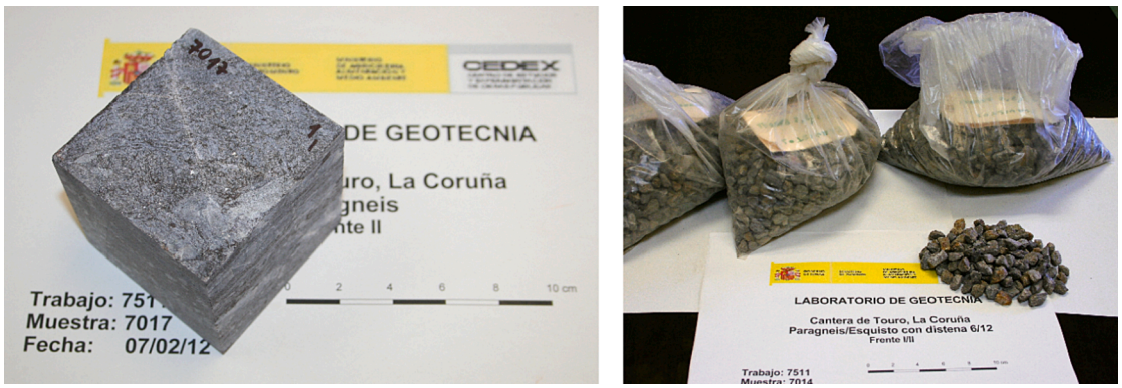

Fig. 3. Examples of a block of schist rock with dimensions 7 × 7 × 7 cm on the left and schist aggregates with particle size 6/12 mm on the right.

main banding of the rock (Fig. 3e) and were sometimes filled with salt precipitated during the test.

After the thermal stress cycles, rock samples of schist rapidly changed to reddish colors because of the oxidation of sulfides and possible oxides present in the rock, which has a greater intensity in the light domains and in prior fissured areas (Fig. 3c). The pre-existing fissures of the schist were re-opened during the tests, especially those parallel to the main foliation of the rock. Equally, these fissures are commonly associated with mineral oxidation processes due to their reddish color (Fig. 3c). Locally, some fissures are also filled with NaCl crystallized during the test. The precipitated NaCl that is also located on schist surface favors its disintegration. Contrarily, rock samples of amphibolite locally changed their color in pre-existing fissures that re-opened during the test where some oxidation processes occurred. However, it was also observed that the opening of new fissures that cross the original texture of the rock and have more irregular shapes than the pre-existing ones. These new fissures are also associated with oxidation processes, as well as local NaCl precipitation.

After durability tests, schist and amphibolite aggregates showed similar deterioration processes to the described in rock specimens (Fig. 4).

After the freeze–thaw test, the schist aggregate (Fib. 4a) showed some oxidation processes, changing their color to reddish tones in the first cycles (Fig. 4b). Although no fissures are visible, some areas with crystallized NaCl were detected in some particles of the aggregates after the test. In the case of amphibolite aggregate (Fig. 4d), the sample showed some oxidation processes without visible fissures (Fig. 4e). Equal to the schist aggregate, some NaCl precipitated on the amphibolite aggregate's surface after the freeze–thaw test.

After the thermal stress test, the schist aggregate showed an intense oxidation with reddish and red surfaces (Fig. 4c). It was also observed that the particles of these aggregates disintegrated and broke up when handled. Amphibolite aggregates were also rapidly and intensively oxidated (Fig. 4f). However, after the tests, no visible fissures were found, only some surface areas where NaCl crystallized.

In addition, to the visual inspection of the samples, the weight loss due to durability tests in both types of samples, rock and aggregates, and lithologies, schist and amphibolite, are registered in Table 3 and Fig. 5.

In Table 3, it can be observed that the weight loss by both lithologies in rock form is minimal compared to its aggregate form, especially in

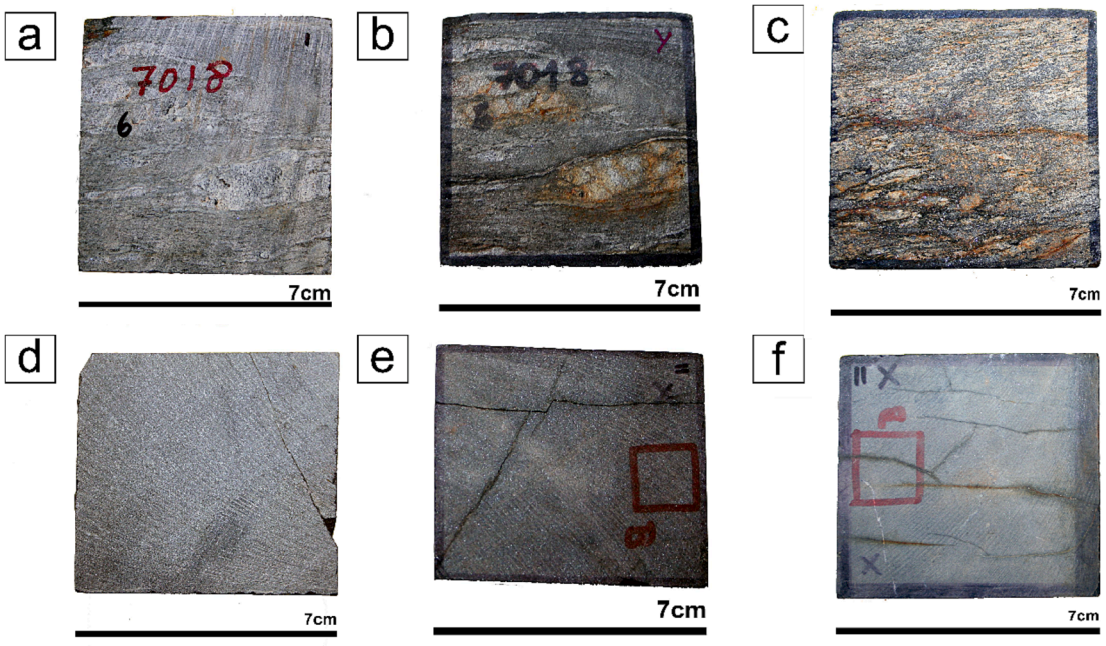

Fig. 4. Examples of samples of schist rock before (a) and after the freeze–thaw test (b) and thermal stress (c) and amphibolite before (d) and after the freeze–thaw test (e) and thermal stress (f). Note the schist sample before the test (a) and the color change and opening of cracks after the cycles (b and c). In amphibolite, before the test (d), small fissures could be observed that increased in size after the freeze–thaw cycles (e) and presented associated mineral oxidation processes in thermal stress tests (f).

Table 3
Average weight loss of rock and aggregate's samples.

Type of sample	Test	N	Weight loss (%)	
			Schist	Amphibolite
Rock	Freeze-thaw	4	0.02 ± 0.02	−0.03 ± 0.02
	Thermal stress	4	0.24 ± 0.23	−0.03 ± 0.02
Aggregate	Freeze-thaw (10/14)	1 (2 kg)	0.48	0.23
	Freeze-thaw (6/12)	1 (2 kg)	0.83	0.41
	Thermal stress (10/14)	1 (2 kg)	3.92	0.56
	Thermal stress (6/12)	1 (2 kg)	5.26	0.64

amphibolite, where there is a slight increase of the weight in its rock form, probably due to NaCl crystallization inside its pores. After both tests, the schist is the material most affected by the durability tests, especially by thermal stress in its aggregate form.

To assess the evolution of weight loss regarding the processing of the materials in the quarry, this parameter has been represented for both lithologies and forms, rock and aggregate, after both durability tests, freeze-thawing and thermal stress (Fig. 5). In addition, to evaluate the effect of crushing processes in the durability of aggregates samples, the weight loss from bigger size aggregates, 10/14, has been added. It can be observed that there is a similar increasing trend in all the samples regarding their processing, sizing, and environmental conditions selected. However, to assess an experimental model of the effect of these processing, sizing, and environmental conditions, more data are required, such as more lithologies or grain size distributions. Equally, it must be highlighted that the schist is the material most affected by the durability tests, especially thermal stress.

3.1. Water absorption coefficient

The results of the water absorption coefficient (C_{Abs}), relative density (d_r), and open porosity (P_w) of the samples that were untreated and treated in the laboratory with the durability tests are shown in Table 4 and Fig. 6.

In Table 4, it can be observed that the water absorption coefficient, and then, the open porosity to water of both lithologies increase after crushing processes in the quarry. Therefore, aggregates, which have a greater porosity than the rock, are more affected by the durability tests. This evolution in the water absorption coefficient regarding samples processing, particle size distribution, and environmental conditions is shown in Fig. 6. In this figure, it also can be observed that both lithologies follow similar trends, although schist is the material most affected by durability tests, especially thermal stress. After the freeze–thaw test, the water absorption coefficient of schist and amphibolite increases in a similar manner. After this test, the water absorption coefficient of schist and amphibolite rises to approximately 1.4–2 times its value (Table 4, Fig. 6). Equally, after the thermal stress test, the water absorption coefficient similarly increases in both lithologies. After this test, the water absorption coefficient can reach 1.5–2.6 times its value (up to 4 for the rock, Table 4, Fig. 6).

3.2. Mercury porosimetry

Results from mercury porosimetry of rocks and aggregates are shown in Tables 5 and 6, respectively. In addition, pore size distribution of the samples regarding their treatment in the laboratory are shown in Fig. 7.

Untreated schist in its rocky form (Fig. 7a) has a total porosity to mercury of 0.95 % (Table 5). Most of the pore sizes are below 5 μm in pore diameter (74.2 %, Table 5 with the most frequent range within 0.1–1 μm (>20 %, Fig. 7a). By contrast, untreated schist aggregate has a total porosity to mercury of 1.29 % (Table 6). Most of the pore sizes are, equally, below 5 μm in pore diameter (>63 %), with the most frequent range between 0.1 and 0.5 μm (16 %, Fig. 7a). However, compared to schist rock, the aggregate shows a slight increase in its porosity, mainly

Fig. 5. Examples of schist 6/12 aggregate (a–c) and amphibolite 6/12 aggregate (d–f), before (a and d) and after the freeze–thaw (b and e) and thermal stress (c and f) tests [50].

Table 4
Average water absorption coefficient, relative density and open porosity measured for both lithologies.

			C_{Abs} (%)		d_r (g/cm^3)		P_w (%)	
Type of sample	Test	N	Schist	Amphibolite	Schist	Amphibolite	Schist	Amphibolite
Rock	Untreated	4	0.35 ± 0.13	0.02 ± 0.01	2.80 ± 0.02	3.11 ± 0.00	0.95 ± 0.36	0.07 ± 0.03
	Freeze-thaw	4	0.35 ± 0.04	0.04 ± 0.01	2.79 ± 0.03	3.10 ± 0.00	0.96 ± 0.11	0.12 ± 0.04
	Untreated	4	0.40 ± 0.12	0.02 ± 0.00	2.81 ± 0.03	3.11 ± 0.00	1.10 ± 0.33	0.07 ± 0.01
	Thermal stress	4	0.49 ± 0.20	0.08 ± 0.03	2.81 ± 0.03	3.11 ± 0.00	1.34 ± 0.53	0.24 ± 0.10
Aggregate	Untreated	1 (2 kg)	1.01	0.62	2.83	3.08	2.79	1.87
	Freeze-thaw (10/14)	1 (2 kg)	1.37	1.02	2.79	3.10	3.66	3.06
	Freeze-thaw (6/12)	1 (2 kg)	1.78	1.22	2.83	2.96	4.79	3.50
	Untreated	1 (2 kg)	0.93	0.43	2.89	3.09	2.57	1.31
	Thermal stress (10/14)	1 (2 kg)	1.90	0.91	2.95	3.10	5.32	2.73
	Thermal stress (6/12)	1 (2 kg)	2.55	1.61	2.84	2.95	6.87	4.52

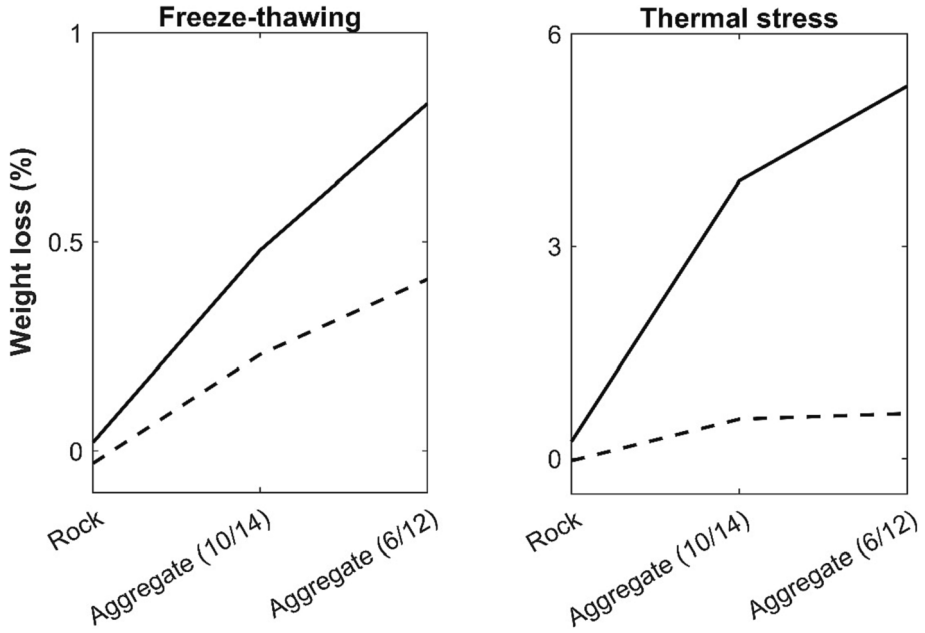

Fig. 6. Representation of the average weight loss of both lithologies subjected to the durability tests regarding samples processing in the quarry. Samples with particle size distribution bigger to 6/12 (10/14) has been added to evaluate the evolution of the materials also regarding their size.

Table 5
Mercury porosimetry parameters of the rocks used before and after durability tests.

	ROCK					
	Untreated		Freeze-thaw		Thermal stress	
	Schist	Amphibolite	Schist	Amphibolite	Schist	Amphibolite
Open porosity (%)	0.95	0.27	1.02	0.29	2.32	0.27
Micro* <5 μm (%)	74.2	15.7	55.1	5.5	74.0	17.9
Macro** >5 μm (%)	25.8	84.3	44.9	94.5	26.0	82.1
Sa***(m^2/g)	0.11	0.001	0.12	0.001	1.51	0.001
Mean pore size (μm)	0.12	4.37	0.12	16.30	0.17	2.90
Tortuosity (μm)	5.99	5.13	2.32	2.60	4.66	2.44

*Micro = Microporosity; **Macro = Macroporosity; ***SSA = Specific surface area.

linked to the increase in its macroporosity (25.8 % rock and 36.8 % aggregate, Tables 5 and 6). Also, pore shape in both forms, rock and aggregate, are irregular and sinuous compared with amphibolite (Table 5 and 6). It is also noticeable that the capillary connections are quite regular in both forms, rock and aggregate, as their tortuosity values are very close to 1 (straight connection fissures). Equally, these capillary connections become slightly more irregular in the aggregate form than the rock form (Tables 5 and 6).

Untreated amphibolite in its rocky form has a very low total porosity to mercury (0.27 %, Table 5), with most of the porosity detected above 5 μm in pore diameter (84.3 %, Table 5). Its most frequent pore diameter range is between 100 and 500 μm (>15 %), followed by the interval 10–50 μm (Fig. 7a). On the contrary, untreated aggregate of amphibolite has a higher total open porosity to mercury (0.42 %, Table 6). In this aggregate, microporosity increases to 58 %, as well as macroporosity (42 %, Table 6), being both porosities similarly relevant. The most

Table 6
Mercury porosimetry parameters of the aggregates before and after the durability tests.

	AGGREGATE					
	Untreated		Freeze-thaw		Thermal stress	
	Schist	Amphibolite	Schist	Amphibolite	Schist	Amphibolite
Open porosity (%)	1.29	0.42	5.96	0.14	3.15	0.27
Micro* <5 μm (%)	63.2	58.0	66.7	47.1	73.3	22.9
Macro** >5 μm (%)	36.8	42.0	33.3	52.9	26.7	77.1
SSA***(m^2/g)	0.17	0.004	0.34	0.001	0.25	0.002
Mean pore size (μm)	0.16	1.24	0.27	1.69	0.32	2.53
Tortuosity (μm)	9.74	4.67	4.71	8.13	5.14	5.83

*Micro = Microporosity; **Macro = Macroporosity; ***SSA = Specific surface area.

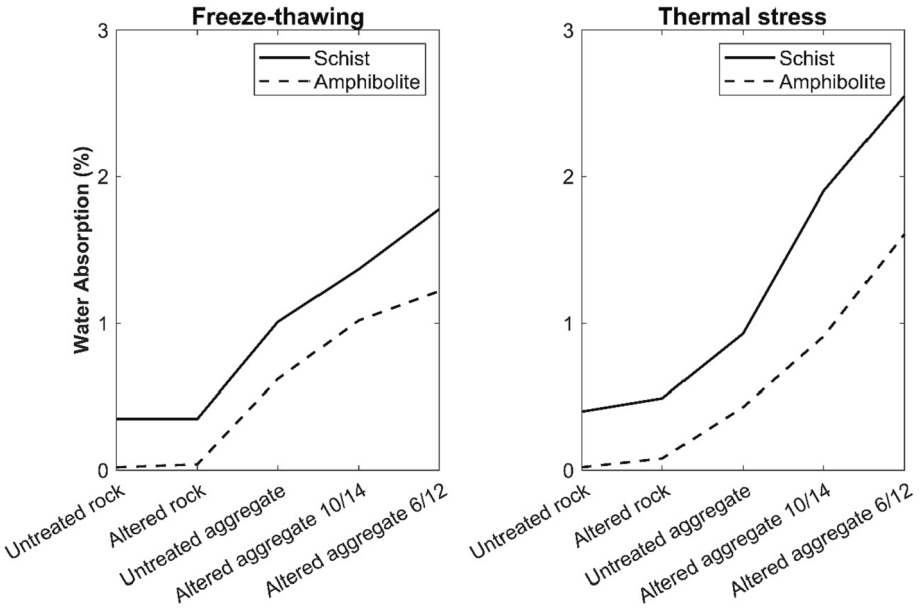

Fig. 7. Representation of the average water absorption coefficient of both lithologies subjected to freeze–thaw and thermal stress tests, regarding their processing in the quarry. Samples with particle size distribution bigger to 6/12 (10/14) have been added to evaluate the evolution of the materials also regarding their size.

frequent pore size interval is between 1 and 5 μm (20 %, Fig. 7a). In both states, rock and aggregate, untreated amphibolite shows regular pores with a low specific surface area, as well as high pore diameters regarding schist samples. Equally, capillary connections are very regular and straight (tortuosity ≈ 1, Tables 5 and 6) as it occurred in schist samples.

After the freeze–thaw test of schist in its rocky form, the sample does not significantly change its total porosity to mercury (from 0.95 to 1.02 %, Tables 5). Although pore diameters ranging from 0.01 to 0.1 μm are still the most frequent (>20 %, Fig. 7b), there is a significant decrease of the microporosity with the corresponding increase of the macroporosity (Tables 5). In addition, the shape of the pores barely varies, making the capillary connections less sinuous and straight (tortuosity from 6 to 2 μm, Table 5). By contrast, the total porosity to mercury of schist aggregates significantly increased after the freeze–thaw test (from 1.29 to 5.96 %, Table 6), being still dominant the microporosity (66.7 %, Table 6), as it occurred in the untreated aggregate. However, it is noticeable that, after the test, pore sizes increased from 0.1 to 0.5 μm (Fig. 7a) to 1–10 μm, where 0.1–1 μm was the most dominant range (Fig. 7b). Additionally, the pores became more irregular, increasing their specific surface area from 0.17 to 0.34 m^2/g (Table 6) and their pore diameter from 0.16 to 0.27 μm (Table 6). Also, the capillary connections became more regular and straight (tortuosity from 9.74 to 4.71 μm, Table 6). Contrarily, after the freeze–thaw test, the internal structure of the amphibolite did not significantly change (Table 5). Macroporosity is still dominant, with pore sizes ranging between 100 and 500 μm (>20 %, Fig. 7b). It can be noticed that the capillary connections between the pores became more regular and straight after the test (tortuosity from 5.13 to 2.44 μm, Table 5). However, in the amphibolite aggregate, total porosity to mercury decreased (from 0.42 to 0.14 %, Table 6), with macroporosity still dominant regarding its untreated form (Fig. 7b). The specific area of the pores did not significantly vary after the test (Table 6), although the capillary connections became more irregular and sinuous (tortuosity from 4.67 to 8.13 μm, Table 6).

After the thermal stress test, the total porosity to mercury of the schist in its rocky form increased from 0.95 to 2.32 % (Table 5), although microporosity is still dominant as it occurred before performing the test. The most common pore diameter range was between 0.01 and 0.1 μm (>30 %, Fig. 7c). However, it can be highlighted that the pores became more irregular (specific surface area from 0.11 to 1.51 m^2/g, Table 5) while capillary connections became slightly straighter (tortuosity from 5.99 to 4.66 μm, Table 5). Equally, in its aggregate form, the total porosity to mercury of the schist increased from 1.29 to 3.15 % (Table 6), as well as its microporosity (73.3 %, Table 6). Thus, the most common ranges of pore diameter are the intervals of 0.1–1 μm and 1–5 μm (>10 %, Fig. 7c). Also, the pores became more irregular (larger specific surface area, 0.17 to 0.25 m^2/g, Table 6), but their capillary connections were more regular and straight (tortuosity from 10 to 5 μm, Table 6). By contrast, after the thermal stress test, the internal structure of amphibolite in its rock form did not significantly change (Table 5). However, it is noticeable that the capillary connections became more regular (tortuosity from 5.13 to 2.44 μm, Table 5). On the other hand, in the amphibolite aggregate, the microporosity was

reduced from 58 to 22.9 % (Table 6), where the most frequent pore diameter ranges were between 10 and 100 and 100–500 μm (Fig. 7c). In addition, the pores were still regular after the test, although they showed higher pore diameters and the capillary connections were slightly more irregular than the rock form (Tables 5 and 6).

3.3. Polarized light optical (OM) and fluorescence microscopy (FM)

The analysis of the schist under OM shows that this lithology has a lepido-granoblastic texture and medium to coarse grain sizes (Fig. 8a). The main mineralogy detected is quartz, plagioclase, biotite, muscovite, garnet, and kyanite. Other secondary minerals observed are zircon, tourmaline, apatite, and some opaque minerals such as sulfides (0.2 %, Table 7). These minerals are distributed in two well-differentiated domains, a quartz-plagioclase domain, and a micaceous domain, which constitute the foliated structure of this rock and, consequently, the aggregates. It is also noticeable that plagioclases are locally degraded to sericite and associated with apatite. In the micaceous domain, composed mainly of biotite and muscovite, the biotite present pleochroic halos due to the existence of zircons. Also, some scattered tourmalines have been observed and are associated with muscovite. In addition, idiomorph to sub-idiomorph garnets both appear in isolated and in aggregates, following the main foliation of the rock.

Under FM, rock schist shows initial intergranular fissures related to

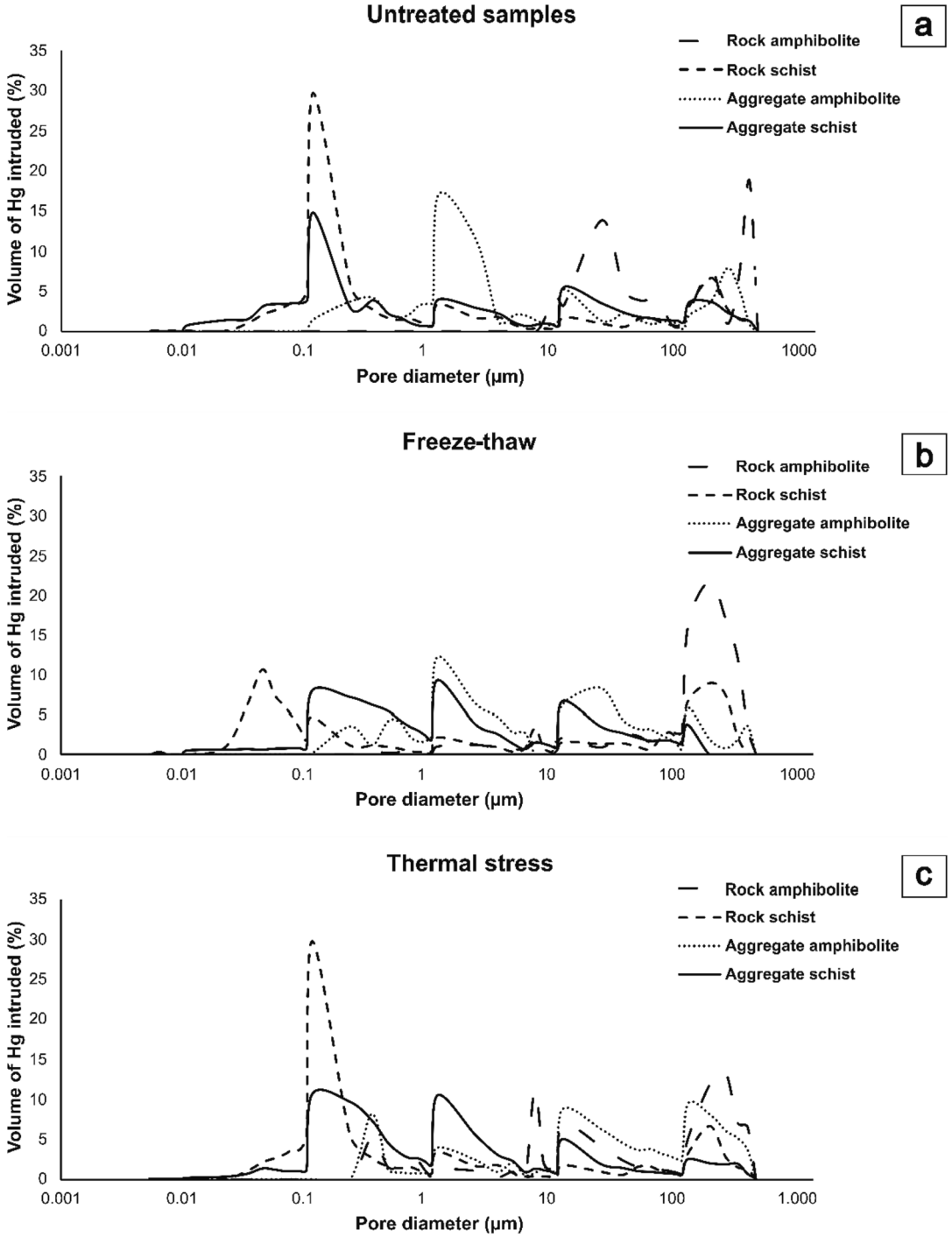

Fig. 8. Pore size distribution of amphibolite and schist untreated samples (a) and exposed to freeze–thaw (b) and thermal stress (c) tests.

Table 7
Chemical composition of the lithologies (schist and amphibolite) studied [78].

Rock type	Oxide content (%)																		
	Al	Ca	Fe	K	Mg	Mn	Na	P	S	Si	Ti	Ba	Cr	Pb	Sr	Zn	Zr	Cl	F
Schist	**16.3**	1.1	6.8	3.4	2.5	0.1	2.5	0.1	**0.2**	**64.0**	0.1	0.07	X	X	0.01	0.01	0.02	X	0.3
Amphibolite	**11.7**	**18.8**	**12.1**	0.1	**5.9**	0.2	1.2	0.1	**2.0**	**41.7**	1.5	0.03	0.01	X	0.01	0.01	0.01	X	0.1

the micaceous domains of the rock (Fig. 8a). These fissures have millimeter lengths and micron thicknesses (≈100 μm). They are usually located on the boundaries between the micaceous domain and the quartz-plagioclase domain. In general, they are not very abundant (<1%). Conversely, under FM, schist aggregate (Fig. 8b) shows the cracking of the micaceous minerals at the surface edges of the aggregate particles (0.2–0.5 mm deep), the opening of a new intragranular porosity of a few microns related to the fracturing of the garnets and muscovite aggregates, and the enlargement of the initial intergranular fissures related to the contact between the micas and the quartz/plagioclase domain detected on the rocky form, reaching millimeter lengths (up to 2 mm).

Amphibolite under OM shows a nematoblastic texture with fine to very fine grain sizes (Fig. 8c). The main minerals of this lithology are plagioclase and amphiboles (actinolite/hornblende), which are responsible for the oriented structure of the rock and, consequently, the aggregates. Secondly, clinozoisite, epidote, calcite, and some opaque minerals (2 % sulfides, Table 7) can be observed. Plagioclases appear in disseminated and forming aggregates, while clinozoisite mineralize some veins with thickness <1 mm that cross the main foliation of the

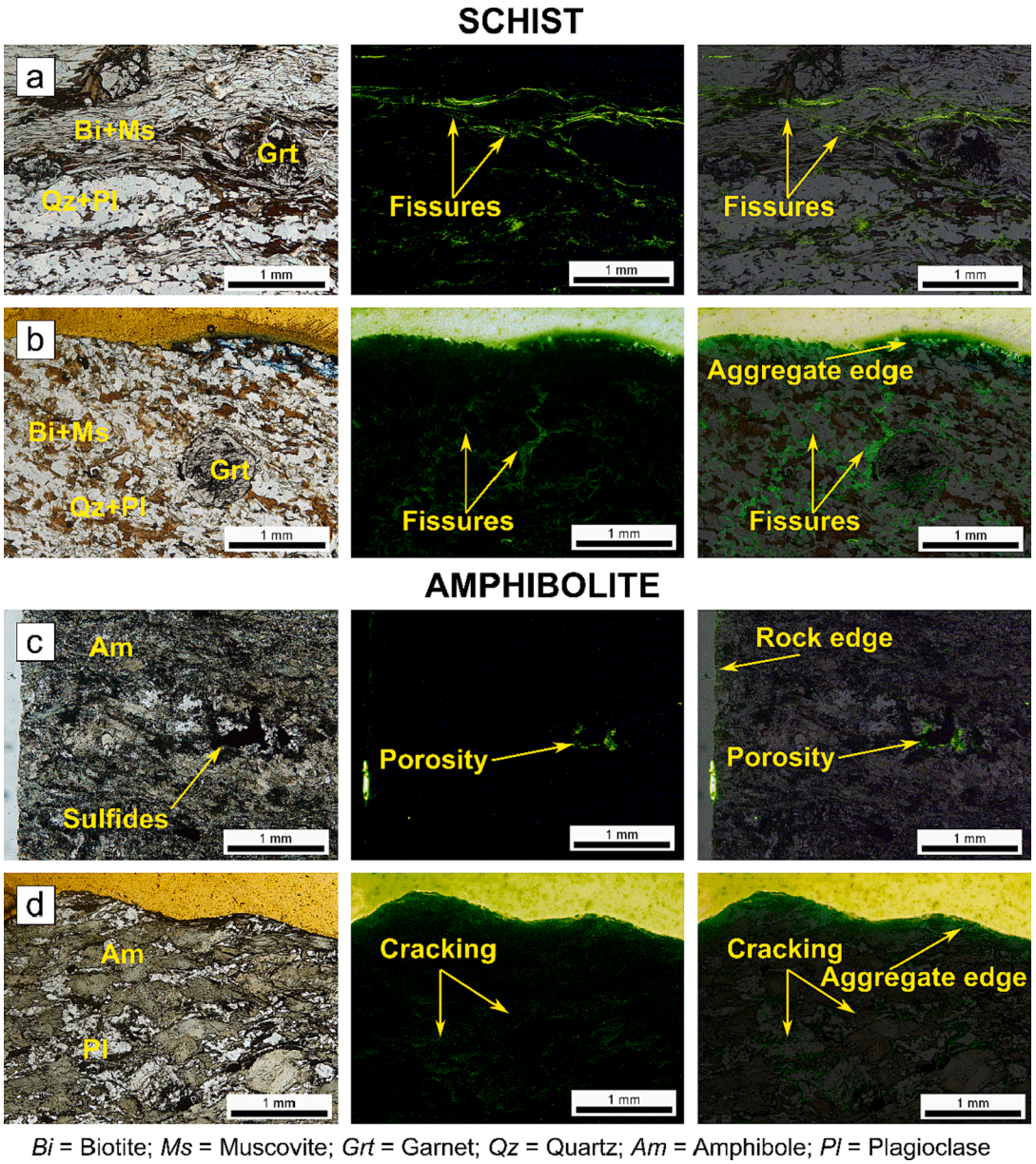

Fig. 9. From left to right, polarized light optical microscope image, fluorescence microscope image and combined optical and fluorescence microscope image of untreated schist in its rock (a) and aggregate (b) forms and untreated amphibolite in its rock (c) and aggregate (d) forms.

rock in different directions. Calcite usually appears in degraded forming aggregates in rock matrix or filling crossing and thin veins (<1 mm) as clinozoisite. Some sulfides also have been detected scattered in rock matrix or related to clinozoisite and calcite veins.

Under FM, amphibolite rock shows, very locally, the presence of intragranular porosity related to the dissolution of the sulfides present in this lithology (<0.5 %, Fig. 8c). However, in its aggregate form, the minerals of the superficial edges of the aggregate particles of amphibolite are fragmented up to 0.1 mm deep, especially the amphiboles. As it occurs in the rocky form, there is some intragranular porosity (a few μm) related to the alteration of plagioclases and the dissolution of sulfides (Fig. 8d).

After the freeze–thaw test, no significant variation in the mineralogical composition was detected in schist rock or aggregates using OM. However, under FM, schist showed the disintegration of the rock's surface, as well as the fissuring of micas and quartz and the reopening of previous fissures present in the rock (2 % porosity, Fig. 9a). These fissures had a thickness of around 100 μm but were centimeters of length. They began in areas of intergranular weakness, such as the contact between micas and quartz, and they propagated through this area as the freeze–thaw cycles progressed. In case of schist aggregate, the significant fracturing of the surface edges of the particles of aggregate was detected, especially in edges where micas dominated (Fig. 9b). The deterioration of the edges was extended 0.2–0.5 mm inside the aggregate. Related to this edge deterioration, intergranular fissures of millimeter length were also observed toward the interior of the aggregate. These fissures are parallel to the general foliation of the rock where they occurred in the micaceous zones or they propagate through the grain boundaries of the quartz and plagioclase, taking advantage of their fragmentation during the crushing of the rock in the quarry. Finally, these fissures reach the foliation of the rock and mica domain. In addition, the reopening of intragranular porosity associated with the fracturing of garnets and the chemical alteration of sulfides present in the aggregate was observed. Overall, the porosity estimated with this

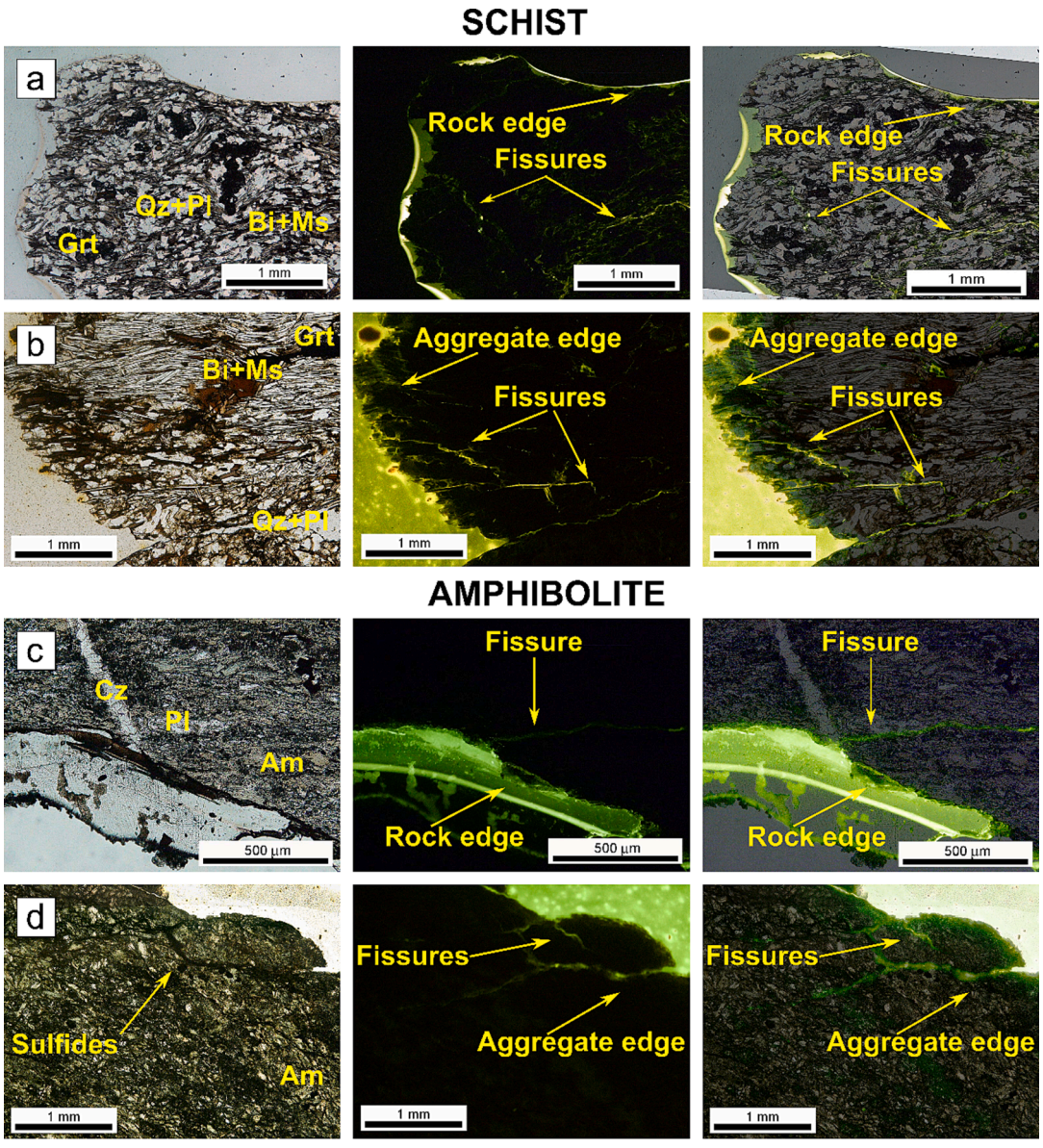

Fig. 10. From left to right, polarized light optical microscope image, fluorescence microscope image and combined optical and fluorescence microscope image of schist in its rock (a) and aggregate (b) forms and amphibolite in its rock (c) and aggregate (d) forms after the freeze–thaw test.

technique was 8 %.

Amphibolite did not show any variation in its mineralogy under OM after the freeze–thaw test. Also, the internal structure variations observed with FM after this test in the rock and were minimal. No significant deterioration was observed, only on the edges and at microscale. Some small fissures related to the mineral alteration of the plagioclases (sericite) were identified (Fig. 9c). Additionally, a slight increase of the intragranular porosity, previously present in the rock, was observed due to the dissolution of sulfides upon contact with the salt brine of the test. Thus, the porosity detected after the test was <1 % using this technique. By contrast, in its aggregate form, the surface edges of the particles of amphibolite aggregates were fractured up to 0.2 mm inside the rock. In addition, new intergranular fissures with millimeter lengths associated with the surface edges of the aggregate (Fig. 9d) were noticed. These fissures also appear to be covered by thin layers of iron oxides due to the chemical alteration of the amphiboles and sulfides during the process. In addition, the reopening of intragranular porosity (few μm) related to plagioclase fracturing by crushing processes was also observed. In general, the porosity detected after the test using this technique was 4 %.

After the thermal stress test, no significant changes in the mineralogical composition of schist were observed under OM. By contrast, under FM, the disintegration of the edges of schist rock was detected, especially in micaceous areas. The opening of new intergranular fissures parallel to the foliation of the rock were also detected. These fissures are thin (≈100 μm) but centimeter long and are associated with the micaceous domain of the rock (Fig. 10a). The formation of cracks related to quartz was also observed, as well as the presence of intragranular porosity related to the dissolution of sulfides present in this lithology. The porosity observed with this technique after the test was 3 %. In its aggregate form, the schist was intensely deteriorated, especially the edges of the particles. Also, the reopening of intergranular fissures with thicknesses up to 0.2–0.3 mm (Fig. 10b) was detected. These fissures practically covered the entire thickness of the aggregate (>4 mm) and began at the particle edges, propagating toward its interior. In general,

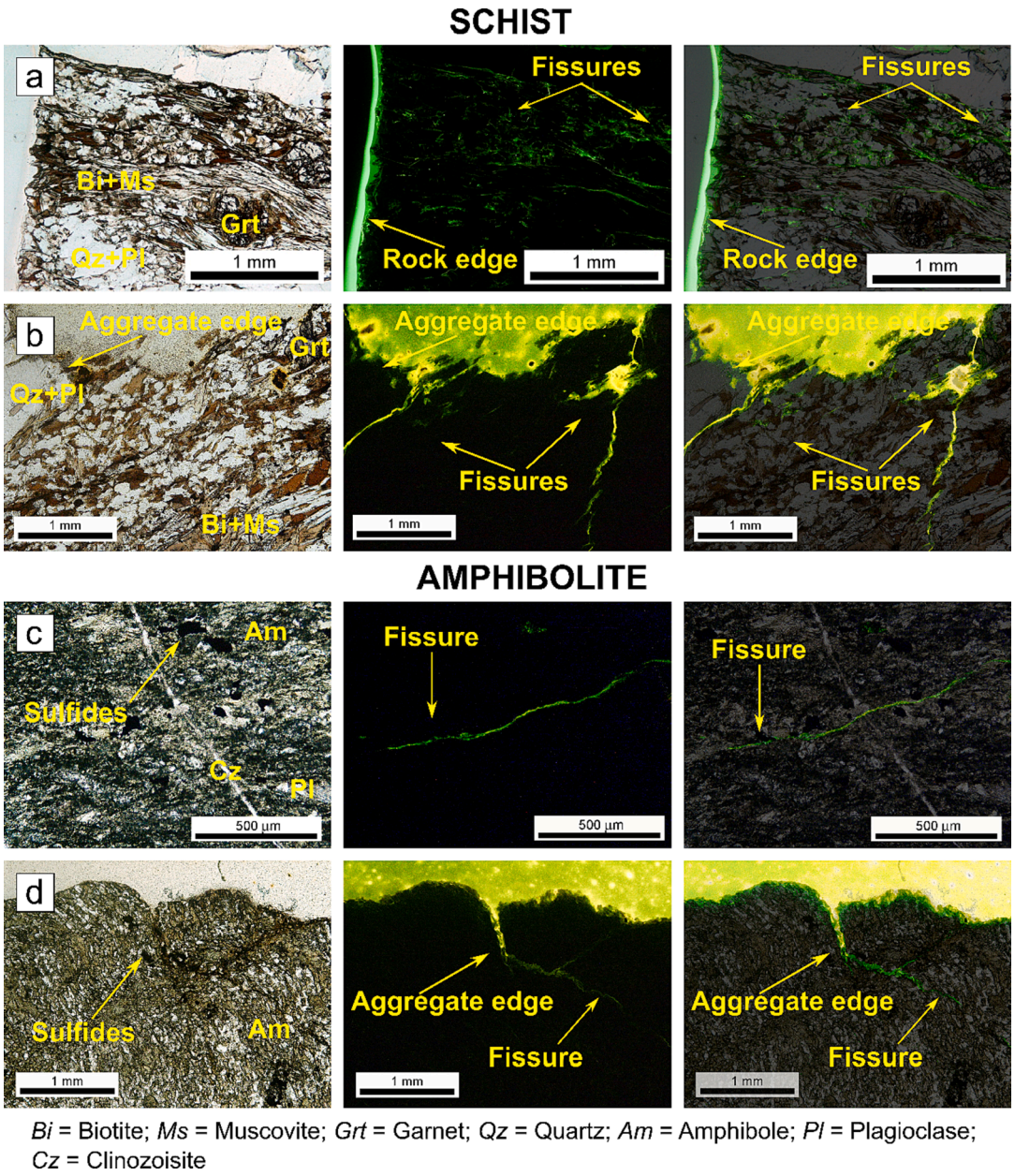

Fig. 11. From left to right, polarized light optical microscope image, fluorescence microscope image and combined optical and fluorescence microscope image of schist in its rock (a) and aggregate (b) forms and amphibolite in its rock (c) and aggregate (d) forms after thermal stress test.

these types of intergranular fissures were parallel to the main foliation of the rock, and they were related to the contact between micaceous and quartz/plagioclase domains (Fig. 10b). Locally, new intergranular fissures were also observed parallel to the main foliation of the rock of significant thickness (0.4 mm) and millimeter lengths related to the quartz veins that crossed the rock. These fissures moved along the edges of the polycrystalline quartz grains, previously fractured during the crushing processes in the quarry. In addition, perpendicular to the main foliation of the rock and with smaller thicknesses, another type of new intergranular fissure was observed. These fissures appeared to be related to the fracturing of the garnets scattered throughout the rock. They had millimeter lengths and could cross the entire particle of aggregate. Finally, the reopening of intragranular porosity was also detected, related to the fracturing of plagioclases and micas by crushing processes or due to the dissolution of sulfides present in the rock. In general, the porosity observed with this technique after the thermal stress test was 15 %.Fig. 11..

In the case of amphibolite, after the thermal stress test, the rock and aggregate samples did not show any variation in their mineralogy under OM. Equally, the effects of the test observed in the rock with FM were minimal. Only at microscale were some fissures detected, parallel to the main orientation of the rock and associated with the sulfides present in the rock (Fig. 10c). Also, the opening of new and short fissures related to clinozoisite and calcite veins that cross the main foliation of the rock was locally detected. The porosity detected after the test with this technique was <1 %. Conversely, in amphibolite aggregate, the particles suffered an intense deterioration at their surface edges, where new intragranular fissures were originated due to the fragmentation of the amphiboles (Fig. 10d). In addition, important oxidation processes related to the alteration of the sulfides present in the rock were detected. The formation of intergranular fissures with millimeter lengths (1–2 mm) and 2–5 μm thicknesses was also observed. These fissures propagate inside the rock following its main foliation (Fig. 10d). Also, the reopening of intragranular porosity inside the aggregate associated with the fracturing of plagioclases by crushing processes was detected. Finally, the porosity generated by the test with this technique was 5 %.

4. Discussion

The visual inspection of the samples analyzed in this work shows that both materials, schist, and amphibolite, are deteriorated by the freeze–thaw and thermal stress tests with NaCl performed in the laboratory. However, the degree of the deterioration observed depends on the lithology, rock processing, and type of test applied. Amphibolite, with the smallest grain size and lower foliation, is less deteriorated than schist by the durability tests done (Table 3). However, in both lithologies, the deterioration increases from rock to aggregate form due to rock processing by crushing in the quarry (Fig. 5). Also, thermal stress is the most damaging test in both schist and amphibolite (Table 3, Fig. 5). Equally, both lithologies tend to similarly increase their deterioration regarding the rock processing, sizing, and the durability tests selected (environmental conditions, Fig. 5). These results agree with the analysis of the evolution of water absorption coefficient, where schist was the most affected by the durability tests (Table 4). Equally, both lithologies similarly increased their water absorption coefficient regarding the rock processing, sizing, and the durability tests selected (Fig. 6). Therefore, although in this work only two lithologies and particle size distributions (10/14 mm and 6/12 mm) have been studied, the finding of similar patterns in weight loss and water absorption coefficient parameters regarding rock crushing and durability tests is promising. In this way, it is proposed for future works the analysis of the evolution of both parameters in function with the durability tests selected, freeze–thaw and thermal stress, in more lithologies and particle size distributions such as 4/8 mm or 14/18 mm. The results from this study may conduct the development of future experimental models that could introduce new insights predicting the quality and durability of rocky materials when they are used as aggregates in construction. It must be highlighted again that this is introductory research to the topic and other parameters such as the increase in the specific surface area exposed to external agents of deterioration of aggregate particles as their size decreases, must be consider for further investigations.

It is also possible to evaluate in more detail the evolution of the internal structure and the mechanisms of deterioration of the rock regarding its crushing in the quarry and durability tests using mercury porosimetry, OM, and FM. After crushing processes in the quarry, the total porosity to mercury increases in both lithologies, especially in schist (Tables 5 and 6). In schist, rock crushing cracks the mineral grains and reopens fissures already present in the stone material, increasing the size of the pores and thus, the macroporosity (Tables 5 and 6). These fissures are especially located on the edge of the aggregate's particles and in the contacts between the micaceous domain and the quartz/plagioclase domain (Fig. 6b). In the case of amphibolite, a new microporosity, non-existent in its rocky form, is formed (Tables 5 and 6). This means that the mechanical cracking of the minerals occurs both on the edges and inside the aggregate. This new microporosity generated corresponds to the cracking of the amphiboles and plagioclases and the alteration of sulfides present in the rock (Fig. 6d).

After freeze–thaw cycles with NaCl, there is an increase of the total porosity to mercury in both lithologies, especially in their aggregate form (Tables 5 and 6). Thus, the deterioration is higher in aggregates due in part to the previous effects of the crushing processes in the quarry and the increase of the specific surface area of the particles exposed to the test, as it has been mentioned above. It must be also highlighted that after the freeze–thaw test, there is a slight increase in the microporosity of the schist aggregate, while the macroporosity increases in the amphibolite aggregate (Fig. 7). Thus, the freeze–thaw deterioration is most superficial in amphibolite, even in its aggregate form. This result is in accordance with the OM and FM analyses. In both lithologies, the surface edges of the aggregate's particles appeared highly deteriorated due to the prior crushing processes in the quarry and, subsequently, to the freeze–thaw test with NaCl carried out in the laboratory. Equally, in both lithologies, new intergranular cracks were produced at the edges of the aggregate that propagated toward its interior since the brine takes advantage of the existing cracked minerals at the edges or preexisting fissures caused by the crushing process (Fig. 8). During the freeze–thaw cycles, this brine penetrates more and more into the aggregate, freezing inside and increasing pore pressure, opening the preexistent porosity and fissures, transforming the internal macro and microporosity [50,59,79]. This process was especially intense on schist aggregate in areas with high proportion of mica minerals and in the contacts between the micaceous domain and the quartz/plagioclase domain, where the fissures produced by the test were >2.5 mm in length (Fig. 9b). By contrast, in the amphibolite aggregate, the deterioration is focused on its particle's edges, where the fissures had lengths <1.5 mm (Fig. 9d).

After the thermal stress cycles with NaCl, there is also an increase of the total porosity to mercury in both lithologies and, again, it is more visible in their aggregate form, especially in schist. Equally, the evolution of porosity was similar in both lithologies observed after the freeze–thaw test. While microporosity increased in the schist aggregate, macroporosity increased in the amphibolite aggregate (Fig. 7). Thus, the effects of the thermal stress test are deeper in the schist aggregate than in the amphibolite aggregate, where the deterioration is more superficial. These results are also in accordance with the OM and FM analyses. Both lithologies were deteriorated by the thermal stress tests with NaCl, especially the schist aggregate (Fig. 10). Equally, the surface edges of both types of aggregates are highly deteriorated due to the previous processes of crushing in the quarry and, subsequently, to the durability test done in the laboratory. In both aggregates, the edges are cracked and new fissures related to the breakage of the edge minerals are formed as a result of the evaporation of the brine and the precipitation of the salt inside the aggregate during the hottest days in summer, causing a greater breakage of the superficial minerals [50,55,59]. In new rainy

periods, the crystallized salt dissolves again and a more concentrated brine is generated, which is introduced through the areas of weakness of the aggregate, deteriorating it even more. The cyclical repetition of this process causes the propagation of the fissures inside the material. Therefore, in the schist aggregate, where mica domains are intensely cracked and fissured due to the crushing processes in the quarry, brine infiltration is deeper than in the amphibolite aggregate (Fig. 10). The schist aggregate shows fissures with lengths longer than 4 mm related with mica domains and their contact with quartz/plagioclase domain while the fissures detected on the amphibolite aggregate do not exceed 1.5 mm in length.

Therefore, according to mercury porosimetry and especially the OM and FM results, the internal structure of both lithologies is affected by crushing processes. The aggregate's edges are cracked. generating new porosity and fissures. Although this mineral cracking is beneficial to some properties of the aggregates, such as their surface roughness and thus, their skid resistance [50], some lithologies such as schist analyzed in this work can be negatively affected by crushing processes in determined environmental conditions [59] in the long-term. Thus, a more in-depth research about crushing processes on aggregates is proposed here for future investigations.

Finally, it must be highlighted that both lithologies were more deteriorated by thermal stress cycles. Specifically, after the thermal stress cycles, the weight loss of the 6/12 mm schist aggregate was 5.3 % (Table 3). Current Spanish regulations of aggregates used on road surfaces do not establish any limit to this test and conditions. Thus, using the limit value assessed for the freeze–thaw test in roads subjected to Atlantic-type climates such as the one supported by the studied materials, 2 % [34], this aggregate would not be resistant to the effects of high temperatures, precipitation, and salt (NaCl). Equally, after the thermal stress cycles, the water absorption coefficient of schist aggregate was 2.55 % (Table 4). Thus, if the limit value of the absorption coefficient established to measure frost resistance of the aggregate were used (maximum limit of 2 %, [34], this aggregate would not be completely resistant to the combined action of salt (NaCl), precipitation and high temperatures. Therefore, it is recommended to consider this test and establish limits to thermal stress deterioration in the aggregates used on roads, especially in the unfortunate present context where heat waves are more frequent due to deforestation and global warming in Spain [52,54,80].

5. Conclusions

The analysis of the evolution of the internal structure of two types of rocks, schist and amphibolite, regarding crushing and sizing processes in a quarry and the effects of freeze–thaw and thermal stress durability tests with NaCl, can be summarized as follows:

- The increase of the weight loss and water absorption coefficient in both lithologies, schist and amphibolite, shows similar tendencies respectively regarding their crushing processing, particle size distribution, and durability tests carried out in the laboratory.
- Both lithologies are more deteriorated by the durability tests performed in the laboratory in their aggregate form than in their rock form. This is mainly due to the fact that crushing processes in the quarry deteriorate the edges of the particles of the aggregates, facilitating the infiltration of the NaCl brine inside the rocky material. Additionally, it must be considered in future research and models that the smaller the particle size, the greater the surface exposed to external agents of deterioration.
- The schist aggregate is the material most affected by crushing processes in the quarry and the durability tests done in the laboratory because of its foliation. Micaceous domains and the contact between this domain and the quartz/plagioclase domain are weakness areas where this material is cracked and fissured during crushing processes, facilitating the deterioration caused by the freeze–thaw and thermal stress cycles.
- Thermal stress with NaCl is the most deteriorating test in both lithologies, especially in schist aggregates. Thus, new recommendations and deterioration limits should be addressed in current standard codes in construction, especially in countries like Spain, where deforestation and global warming are increasing heat waves in the summer months.

Finally, although the results obtained in this work are promising, the authors suggest analyzing more lithologies and particle size distributions of rocky aggregates to assess experimental models to simulate the deterioration of a rock from the quarry to its final use in construction and delve into the mechanisms of deterioration of rocks used as aggregates in construction.

CRediT authorship contribution statement

A.P. Pérez-Fortes: Conceptualization, Data curation, Formal analysis, Investigation, Methodology, Writing – original draft, Writing – review & editing. **M.J. Varas-Muriel:** Conceptualization, Investigation, Methodology, Supervision, Validation, Writing – review & editing. **M. Bermejo:** Visualization, Writing – review & editing.

Declaration of Competing Interest

The authors declare that they have no known competing financial interests or personal relationships that could have appeared to influence the work reported in this paper.

Data availability

Data will be made available on request.

Acknowledgements

This research was partly funded through the Community of Madrid under the project S2018/NMT-4372 (TOP-HERITAGE) and the Grant Program from the CEDEX Research Agency (BOE June 27, 2009). Some of the authors are members of Complutense University of Madrid research team 921349. The authors wish to thank Dr. Herminia Cano Linares, Associate Professor at the Technical University of Madrid (UPM) for her support during this project. We also thank the company *Construcciones Francisco Gómez y Cía., S.L*, for the provision of the materials to develop this research. The authors also want to thank to Mr. Matthew S. Rose for the English editing of the text and to the editor and reviewers for their kind suggestions.

References

[1] F. Alonso Rodríguez, R. Esbert Alemany, J. Ordaz Gargallo, P. Vázquez, Análisis del deterioro en los materiales pétreos de edificación, Rev. electrónica ReCoPaR 3 (2006) 23–32.
[2] A. Hartley, A review of the geological factors influencing the mechanical properties of road surface aggregates, Q. J. Eng. Geol. 7 (1) (1974) 69–100, https://doi.org/10.1144/GSL.QJEG.1974.007.01.05.
[3] R. Přikryl, Assessment of rock geomechanical quality by quantitative rock fabric coefficients: Limitations and possible source of misinterpretations, Eng. Geol. 87 (3–4) (2006) 149–162, https://doi.org/10.1016/j.enggeo.2006.05.011.
[4] S. Anastasio, A.P.P. Fortes, E. Kuznetsova, S.W. Danielsen, Relevant petrological properties and their repercussions on the final use of aggregates, Energy Procedia (2016), https://doi.org/10.1016/j.egypro.2016.10.073.
[5] S. Adomako, C.J. Engelsen, R.T. Thorstensen, D.M. Barbieri, Review of the relationship between aggregates geology and Los Angeles and micro-Deval tests, Bull. Eng. Geol. Environ. 80 (3) (2021) 1963–1980, https://doi.org/10.1007/s10064-020-02097-y.
[6] M. Bellanger, F. Homand, J.M. Remy, Water behaviour in limestones as a function of pores structure: application to frost resistance of some Lorraine limestones, Eng. Geol. 36 (1–2) (1993) 99–108, https://doi.org/10.1016/0013-7952(93)90022-5.
[7] A. Saad, S. Guédon, F. Martineau, Microstructural weathering of sedimentary rocks by freeze-thaw cycles: experimental study of state and transfer parameters,

Comptes Rendus – Geosci. 342 (3) (2010) 197–203, https://doi.org/10.1016/j.crte.2009.12.009.
[8] C. Walbert, J. Eslami, A.L. Beaucour, A. Bourges, A. Noumowe, Evolution of the mechanical behaviour of limestone subjected to freeze–thaw cycles, Environ. Earth Sci. 74 (7) (2015) 6339–6351, https://doi.org/10.1007/s12665-015-4658-2.
[9] J. Eslami, C. Walbert, A.L. Beaucour, A. Bourges, A. Noumowe, Influence of physical and mechanical properties on the durability of limestone subjected to freeze-thaw cycles, Constr. Build. Mater. 162 (2018) 420–429, https://doi.org/10.1016/j.conbuildmat.2017.12.031.
[10] Y. Liu, Y. Cai, S. Huang, Y. Guo, G. Liu, Effect of water saturation on uniaxial compressive strength and damage degree of clay-bearing sandstone under freeze-thaw, Bull. Eng. Geol. Environ. 79 (4) (2020) 2021–2036, https://doi.org/10.1007/s10064-019-01686-w.
[11] A. La Iglesia, V. González, V. López-Acevedo, C. Viedma, Salt crystallization in porous construction materials I estimation of crystallization pressure, J. Cryst. Growth 177 (1–2) (1997) 111–118, https://doi.org/10.1016/S0022-0248(96)01072-X.
[12] G.W. Scherer, Stress from crystallization of salt, Cem. Concr. Res. 34 (9) (2004) 1613–1624, https://doi.org/10.1016/j.cemconres.2003.12.034.
[13] D. Benavente, J. Martínez-Martínez, N. Cueto, M.A. García-del-Cura, Salt weathering in dual-porosity building dolostones, Eng. Geol. 94 (3–4) (2007) 215–226, https://doi.org/10.1016/j.enggeo.2007.08.003.
[14] M.F. La Russa, et al., Study of the effects of salt crystallization on degradation of limestone rocks, Period Mineral. 82 (1) (2013) 113–127, https://doi.org/10.2451/2013PM0007.
[15] B. Silva, B. Prieto, T. Rivas, M.J. Sanchez-Biezma, G. Paz, R. Carballal, Rapid biological colonization of a granitic building by lichens, Int. Biodeterior. Biodegrad. 40 (2–4) (1997) 263–267, https://doi.org/10.1016/S0964-8305(97)00051-6.
[16] A. de los Ríos, B. Cámara, M.Á. García del Cura, V.J. Rico, V. Galván, C. Ascaso, Deteriorating effects of lichen and microbial colonization of carbonate building rocks in the Romanesque churches of Segovia (Spain), Sci. Total Environ. 407 (3) (2009) 1123–1134, https://doi.org/10.1016/j.scitotenv.2008.09.042.
[17] A.Z. Miller, et al., Bioreceptivity of building stones: a review, Sci. Total Environ. 426 (2012) 1–12, https://doi.org/10.1016/j.scitotenv.2012.03.026.
[18] D. Vázquez-Nion, B. Silva, B. Prieto, Influence of the properties of granitic rocks on their bioreceptivity to subaerial phototrophic biofilms, Sci. Total Environ. 610–611 (2018) 44–54, https://doi.org/10.1016/j.scitotenv.2017.08.015.
[19] R. Kala, V.D. Pandey, Variable Growth Patterns of Epilithic Cyanobacteria on Different Rocks, *Recent Adv. Sci. with Spec. Ref. to Himalaya*, p. 117.
[20] S.A. Russel, Stone preservation committee report (Appendix I), 1927.
[21] Larson, T. D., & Cady, P. D. (1969). Identification of frost-susceptible particles in concrete aggregates. *NCHRP Report*, (66). Transportation Research Board, Washington, DC, 1969.
[22] P.P. Hudec, Durability of rock as function of grain size, pore size, and rate of capillary absorption of water, J. Mater. Civ. Eng. 1 (1) (1989) 3–9, https://doi.org/10.1061/(ASCE)0899-1561(1989)1:1(3).
[23] M. Ondrášik, M. Kopecký, Rock pore structure as main reason of rock deterioration, Stud. Geotech. Mech. 36 (1) (2014) 79–88, https://doi.org/10.2478/sgem-2014-0010.
[24] L. Smith, M.R.; Collins, *Aggregates: Sand, Gravel and Crushed Rock Aggregates for Construction Purposes*, Geological. London: ciety Engineering Geology Special Pub. No. 9, 1993.
[25] J.E. Kogel, N.C. Trivedi, J.M. Barker, y S.T. Krukowski, *Industrial minerals \& rocks: commodities, markets, and uses*. SME, 2006.
[26] P.G. Fookes, C.S. Gourley, C. Ohikere, Rock weathering in engineering time Naturally occurring weathering processes, Q. J. Eng. Geol. 21 (1988) 33–57.
[27] A.P. Pérez-fortes, Aggregates properties for safety road surfaces, en *Advances in Engineering Research, 40*, Nova Science Publishers, 2020, pp. 103–134.
[28] J.R. Hosking, L.W. Tubey, *Research on Low Grade and Unsound Aggregates*. Road Research Laboratory Report, LR 293, Crowthorne, UK, 1969.
[29] A.B. Dibb, T.E. Hughes, D.W. Poole, Controls of size and shape of natural armourstone, Q. J. Eng. Geol. Hydrogeol. 16 (1) (1983) 31–42, https://doi.org/10.1144/GSL.QJEG.1983.016.01.03.
[30] A. P. Pérez-Fortes, P. Castiñeiras, y M. J. Varas-Muriel, Optimización de la producción de áridos procedentes de canteras con frentes complejos: cantera de Touro, A Coruña (España), *Geogaceta*, vol. 62, pp. 111-114, abr. 2017, [En línea]. Disponible en: http://www.sociedadgeologica.es/archivos/geogacetas/geo62/geo62_28.pdf.
[31] J.T. Tamayo, C.G. Guevara, J.C. Vargas, Estudio de la Degradación de los Agregados Petreos durante la Vida Util de los Pavimentos 5 (2011) 13–21.
[32] I.M. Asi, Evaluating skid resistance of different asphalt concrete mixes, Build. Environ. 42 (1) (2007) 325–329, https://doi.org/10.1016/j.buildenv.2005.08.020.
[33] A.P. Pérez Fortes, S. Anastasio, E. Kuznetsova, S.W. Danielsen, Behaviour of crushed rock aggregates used in asphalt surface layer exposed to cold climate conditions, Environ. Earth Sci. 75 (21) (2016), https://doi.org/10.1007/s12665-016-6191-3.
[34] EN 13043, Aggregates for bituminous mixtures and surface treatments for roads, airfields and other trafficked areas. 2003.
[35] G.B. Pretel, PG-3 Pliego de prescripciones técnicas generales para obras de carreteras y puentes, Ediciones Liteam SL (2019).
[36] E. 933-4, Tests for geometrical properties of aggregates - Part 4: Determination of particle shape - Shape index. 2008.
[37] EN 12697-11, *Bituminous mixtures - Test methods - Part 11: Determination of the affinity between aggregate and bitumen*. 2022.
[38] EN 1367-1, *Tests for thermal and weathering properties of aggregates - Part 1: Determination of resistance to freezing and thawing*. 2008.
[39] E. 1367-5, Tests for thermal and weathering properties of aggregates - Part 5: Determination of resistance to thermal shock. European Committee for Standardization., 2011.
[40] EN 1097-8, *Tests for mechanical and physical properties of aggregates - Part 8: Determination of the polished stone value*. 2021.
[41] M. Räisänen, M. Mertano, An evaluation of the procedure and results of laboratory crushing in quality assessment of rock aggregate raw materials, Bull. Eng. Geol. Environ. 63 (1) (2004) 33–39, https://doi.org/10.1007/s10064-003-0218-1.
[42] M.N. Bouquety, Y. Descantes, L. Barcelo, F. de Larrard, B. Clavaud, Experimental study of crushed aggregate shape, Constr. Build. Mater. 21 (4) (2007) 865–872, https://doi.org/10.1016/j.conbuildmat.2005.12.013.
[43] J. Komba, M.B. Mgangira, L. Mohale, Investigation of the Effects of the Type of Crusher on Coarse Aggregate Shape Properties Using the Three-Dimensional Laser Scanning Technique, pp. 125-132, 2016, doi: 10.1061/9780784480090.016.
[44] B. Rajan, D. Singh, Comparison of shape parameters and laboratory performance of coarse aggregates produced from different types of crushing operations, J. Mater. Civ. Eng. 29 (7) (2017) 04017044, https://doi.org/10.1061/(asce)mt.1943-5533.0001874.
[45] L.M. Diógenes, I.S. Bessa, V.T.F. Castelo Branco, E. Mahmoud, The influence of stone crushing processes on aggregate shape properties, Road Mater. Pavement Des. 20 (4) (2019) 877–894, https://doi.org/10.1080/14680629.2017.1422792.
[46] M. Fladvad, T. Onnela, Influence of jaw crusher parameters on the quality of primary crushed aggregates, Miner. Eng. 151 (2020) jun, https://doi.org/10.1016/j.mineng.2020.106338.
[47] M. Kamani, R. Ajalloeian, The effect of rock crusher and rock type on the aggregate shape, Constr. Build. Mater. 230 (2020), 117016, https://doi.org/10.1016/j.conbuildmat.2019.117016.
[48] C. Wang, H. Wang, M. Oeser, M.R. Mohd Hasan, Investigation on the morphological and mineralogical properties of coarse aggregates under VSI crushing operation, Int. J. Pavement Eng. (2020) 1–14, https://doi.org/10.1080/10298436.2020.1714043.
[49] P.G. Fookes, Geomaterials, Q.J. Eng. Geol. Hydrogeol. 24 (1) (1991) 3–15, https://doi.org/10.1144/GSL.QJEG.1991.024.01.02.
[50] A. P. Pérez-Fortes, M.J. Varas-Muriel, P. Castiñeiras, Long-term behavior of the micro-texture of aggregates used on roads subjected to extreme climate conditions and winter maintenance operations, *Wear*, vol. 474-475, no. May 2020, 2021, doi: 10.1016/j.wear.2021.203757.
[51] C. Yagüe, M. Martija, J. Torres, A. I. Maldonado, y E. Zurita, Análisis estadístico de las olas de calor y frío en España, *Acta las Jornadas Científicas la Asoc. Meteorológica Española*, no. 29, pp. 1-6, 2020, [En línea]. Disponible en: http://www.divulgameteo.es/uploads/Olas-frío-calor.pdf.
[52] A. Izquierdo, M. Manzano, Q. Martín, J. Montero, J. Salazar, Evolución temporal de las olas de calor en la meseta central española, Soc. Española Climatol. (2012) 441–448, entre 1961 y 2010.
[53] R. Carmona, J. Díaz, I.J. Mirón, C. Ortíz, I. León, C. Linares, Geographical variation in relative risks associated with cold waves in Spain: The need for a cold wave prevention plan, Environ. Int. 88 (2016) 103–111, https://doi.org/10.1016/j.envint.2015.12.027.
[54] J. Abaurrea, J. Asín, A.C. Cebrián, Modelling the occurrence of heat waves in maximum and minimum temperatures over Spain and projections for the period 2031–60, Glob. Planet. Change 161 (2018) 244–260, https://doi.org/10.1016/j.gloplacha.2017.11.015.
[55] B. Obika, R.J. Freer-Hewish, P.G. Fookes, Soluble salt damage to thin bituminous road and runway surfaces, Q. J. Eng. Geol. 22 (1) (1989) 59–73, https://doi.org/10.1144/GSL.QJEG.1989.022.01.05.
[56] X. Shi, The use of road salts for highway winter maintenance: an asset management perspective, en *2005 ITE District 6 Annual Meeting*, 2005, pp. 10-13.
[57] X. Shi, M. Akin, T. Pan, L. Fay, Y. Liu, Z. Yang, Deicer impacts on pavement materials: introduction and recent developments, Open Civ. Eng. J. 3 (1) (2009) 16–27, https://doi.org/10.2174/1874149500903010016.
[58] F. Giuliani, F. Merusi, G. Polacco, S. Filippi, M. Paci, Effectiveness of sodium chloride-based anti-icing filler in asphalt mixtures, Constr. Build. Mater. 30 (2012) 174–179, https://doi.org/10.1016/j.conbuildmat.2011.12.036.
[59] A.P. Pérez-Fortes, M.J. Varas-Muriel, P. Castiñeiras, Using petrographic techniques to evaluate the induced effects of NaCl, extreme climatic conditions, and traffic load on Spanish road surfaces, Mater. Constr. 67 (2017), https://doi.org/10.3989/mc.2017.07516.
[60] U. Buschbom, Experiences with de-icing salts in W. Germany, Eur. J. For. Pathol. 10 (6) (1980) 349–353, https://doi.org/10.1111/j.1439-0329.1980.tb00048.x.
[61] L.B. Pedersen, T.B. Randrup, M. Ingerslev, Effects of road distance and protective measures on deicing NaCl deposition and soil solution chemistry in planted median strips, J. Arboric. 26 (5) (2000) 238–245.
[62] H. Iwata, K. Yamamoto, K. Nishiduka, H. Higashi, S. Nakao, Y. Miyazaki, Development of an on-vehicle type salinity measurement sensor for controlling winter roadway surfaces, Int. J. ITS Res. 2 (1) (2004) 297–306.
[63] M. Ruiz-Llata, P. Martín-Mateos, J.R. López, P. Acedo, Remote optical sensor for real-time residual salt monitoring on road surfaces, Sens. Actuat. B Chem. 191 (2014) 371–376, https://doi.org/10.1016/j.snb.2013.10.009.
[64] J.L. Gómez Barreiro, P. Castiñeiras, J.R. Martínez Catalán, R. Arenas, Nueva interpretación petrológica y tectónica de las anfibolitas pobres en calcio del antiforme de Arinteiro (NO del Macizo Ibérico). II: estructura e implicaciones para la génesis de anfibolitas pobres en calcio, Geogaceta 32 (2002) 87–90.
[65] P. Castiñeiras, F.D. García, J.G. Barreiro, REE-assisted U-Pb zircon age (SHRIMP) of an anatectic granodiorite: Constraints on the evolution of the A Silva granodiorite,

Iberian allochthonous complexes, Lithos 116 (1–2) (2010) 153–166, https://doi.org/10.1016/j.lithos.2010.01.013.
[66] EN 932-1, Tests for general properties of aggregates - Part 1: Methods for sampling. 1997.
[67] EN 1097-2, *Tests for mechanical and physical properties of aggregates - Part 2: Methods for the determination of resistance to fragmentation*. 2021.
[68] EN 13755, *Natural stone test methods - Determination of water absorption at atmospheric pressure*. 2008.
[69] EN 1097-6, *Tests for mechanical and physical properties of aggregates - Part 6: Determination of particle density and water absorption*. 2022.
[70] UNE 83134, *Aggregates for concrete. determination of densities, porosity, absorption coefficient and water content in coarse aggregate*. 1990.
[71] D.N. Winslow. Advances in experimental techniques for mercury intrusion porosimetry, in *Surface and colloid science*, Springer, 1984, pp. 259–282.
[72] R.M. Esbert, J. Ordaz, F.J. Alonso, M. Montoto, *Manual de diagnosis y tratamiento de materiales pétreos y cerámicos*. Collegi d'Aparelladors i Arquitectes Tècnics de Barcelona. Barcelona, España, 1997.
[73] ASTM D4404-18, *Standard Test Method for Determination of Pore Volume and Pore Volume Distribution of Soil and Rock by Mercury Intrusion Porosimetry*. 2018.
[74] C. Rodríguez-Navarro, E. Sebastián, Técnica de análisis del sistema poroso de materiales pétreos ornamentales: usos y limitaciones, Rev. Digit. del Cedex no. 96 (1994) 130.
[75] R. Fort, M.J. Varas, M. Alvarez de Buergo, D. Martin-Freire, Determination of anisotropy to enhance the durability of natural stone, J. Geophys. Eng. 8 (3) (2011) S132–S144, https://doi.org/10.1088/1742-2132/8/3/s13.
[76] M.E. Gunter, The polarized light microscope: Should we teach the use of a 19th century instrument in the 21st century, J. Geosci. Educ. 52 (1) (2004) 34–44, https://doi.org/10.5408/1089-9995-52.1.34.
[77] Á. Rodríguez Rey, M. Montoto San Miguel, L. Calleja Escudero, V. Gómez Ruiz de Argandoña, L.M. Suárez del Río, Aplicación de la microscopía óptica de fluorescencia al estudio textural del clínker de cemento portland, Mater. Construcción 37 (205) (1987) 17–22, https://doi.org/10.3989/mc.1987.v37.i205.875.
[78] A.P. Pérez Fortes, Calidad y durabilidad de áridos metamórficos empleados en capas de rodadura gallegas bajo el efecto de la sal y una climatología extrema, p. 460, PhD Thesis, Universidad Complutense de Madrid, Spain. 2016.
[79] T.C. Chen, M.R. Yeung, N. Mori, Effect of water saturation on deterioration of welded tuff due to freeze-thaw action, Cold Reg. Sci. Technol. 38 (2–3) (2004) 127–136, https://doi.org/10.1016/j.coldregions.2003.10.001.
[80] C. Yagüe, M. Martija, J. Torres, A.I. Maldonado, E. Zurita, Análisis estadístico de las olas de calor y frío en España, Acta Jornadas Científicas Asoc. Meteorológica Española 29 (2020) 1–6.